Silver-based coordination polymers assembled by dithioether ligands: potential antibacterial materials despite received ideas

Quentin Gaudillat,[a] Anna Krupp,[b] Thibaut Zwingelstein,[c] Vincent Humblot,[c] Carsten Strohmann,[b] Isabelle Jourdain,[a] Michael Knorr [a] and Lydie Viau*[a]

We report on the first examples on the antibacterial activity towards Gram-negative and Gram-positive bacteria of 2D silver-based coordination polymers obtained by self-assembly with acetylenic dithioethers ligands. Their structure imparts a good stability that allows a sustainable release of Ag^+ in the media.

Silver and silver-based compounds have been routinely used as general antimicrobial agents for over a century.[1, 2] Many silver (I)-based coordination polymers (CPs) or Metal-Organic Frameworks (MOFs) with diverse topologies and dimensionalities have been described based on the abundant coordination geometry of Ag^+ ions. As usually encountered in the synthesis of most CPs and MOFs, the overall architecture depends on many factors like the metal-to-ligand ratio, the nature of the counter-anions, the functionality of the ligands and the experimental conditions. Several silver-based CPs and MOFs exhibit interesting photoluminescence[3-7] and antibacterial properties[8-15] and have been used for the elaboration of nanomaterials.[16-18] The interest in using silver-based CPs or MOFs for antibacterial applications also stems from the fact that they may act as a reservoir controlling the release rate of silver and thus avoiding the toxicity caused by an excess amount of silver. Nomiya *et al* were the first to report the potential antibacterial activity of Ag(I)-based CPs against bacteria, yeast and mold.[19] They synthesized a series of silver-based complexes containing S,[20] O[21] and N[19] ligands and screened their antimicrobial activities. They found that silver complexes containing Ag–N or Ag–O bonds showed more efficient antimicrobial activities than those containing Ag–S bounds. This has been attributed to the relative weakness of Ag–O/N bonds which are easily replaced by biomolecules bearing thiol groups. Their findings are in line with the most frequently reported mechanism responsible for the antibacterial activity of CPs and MOFs, assuming that the release of silver ions into the biological medium is due to degradation of the CP.[22] It appears as such that silver release should be facilitated in the presence of fragile frameworks, i.e., when weak bonds between metal and donor atoms are present. To build-up potentially labile structures, one way is to choose specific ligands according to Pearson's HSAB theory.[23] As such, many examples of antibacterial MOFs and CPs were obtained by coordination of the soft Lewis acid Ag(I) to hard bases such as carboxylate[24, 25] or intermediate soft/hard bases such as nitrogen-containing ligands.[9, 10, 26-32] Mono- and dithioethers ligands, on the other hand, can be regarded as soft bases. Particularly, dithioethers ligands have been used as building blocks for the assembly of CPs using soft M(I) coinage metals ions. Especially, several groups, including ours, have been interested in the formation of Cu(I)-based CPs[33-36] while the groups of Bu and Kim have investigated the formation of Ag(I)-based CPs.[37-41] However, we are not aware of any study related to the antibacterial activity of such Ag(I)-based CPs assembled by dithioethers ligands. Therefore, we present herein the synthesis, the X-Ray characterization, and antimicrobial properties of two coordination polymers **CP1** $[Ag_2(\mathbf{L1})][(NO_3)_2]_n$ and **CP2** $[Ag(\mathbf{L2})][(NO_3)]_n$ obtained by the self-assembly of acetylenic dithioethers $RSCH_2C{\equiv}CCH_2SR$ (R = Ph **L1**, R = C_6H_{11} **L2**) ligands with $AgNO_3$. The acetylenic function was chosen *i*) to provide structural rigidity and *ii*) to probe its potential as π-coordination site. **CP1** was prepared by reaction of $AgNO_3$ with **L1** using a 2:1 molar ratio in a methanol/chloroform solvent mixture (Scheme 1). Attempts to obtain a different architecture using a 1:1 ratio failed and led only to the formation of **CP1** as checked by PXRD (Fig. S16). However, using **L2** where the bulkier cyclohexyl substituent replaces the phenyl group, we succeeded to isolate **CP2** by reaction with two equivalents of $AgNO_3$ in acetonitrile (note that **CP2** could not be isolated in a 1:1 ratio). The elemental analysis of the product formed confirmed an $AgNO_3$**L2** composition. Both **CP1** and **CP2** were found to be air stable over several months.

[a] *Institut UTINAM, UMR CNRS 6213, Université de Franche-Comté, 16 route de Gray, 25030 Besançon Cedex.*
[b] *Anorganische Chemie Technische Universität Dortmund, Otto-Hahn* Straße 6, 44227 Dortmund, Germany.
[c] *Université Franche-Comté, UMR CNRS 6174, Institut FEMTO-ST, 15B avenue des Montboucons, 25030 Besançon, France.*
† Footnotes relating to the title and/or authors should appear here.
Electronic Supplementary Information (ESI) available: [details of any supplementary information available should be included here]. See DOI: 10.1039/x0xx00000x

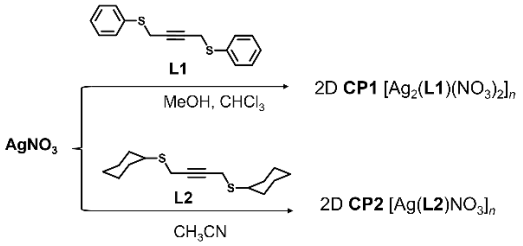

Scheme 1 Reaction of **L1** and **L2** with $AgNO_3$ to afford **CP1** and **CP2**.

CP1 $[Ag_2\mathbf{L1}(NO_3)_2]_n$ crystallizes in the monoclinic $P2_1$ space group. Crystallographic data are given in Table S1 and selected interatomic distances are presented in Table S2 (see ESI†). The crystal structure of **CP1** reveals that the asymmetric unit contains two crystallographically different silver ions, one **L1** molecule and two nitrate anions (Fig. S9). Ag1 and Ag2 are five-coordinated to two S atoms from distinct ligands and to one monodentate and one bidentate nitrate ions in a AgS2O3 coordination mode with classical *d*Ag–O distances ranging from 2.502(4) Å to 2.638(4) Å and *d*Ag–S distances ranging from 2.5346(12) to 2.5704(12) Å (Table S2). The fact that all Ag–S and Ag–O distances fall approximately within the same range ≈2.5 Å despite the larger atomic radii of the sulphur atoms *vs. oxygen* clearly demonstrates that the Ag–S bonds can be considered as stronger than the Ag–O bonds. The nitrate anions are tridentate bridging two Ag atoms in mono- and bidentate fashions respectively to form polymeric Ag2–O–N–O–Ag1 1D chains extending in the *c* direction. In this structure, each **L1** ligand is connected to four different silver centres via bis(μ_2-S) mode leading to the formation of zigzagging Ag1–S1–Ag1–S1–Ag1 and Ag2–S2–Ag2–S2–Ag2 chains running perpendicularly to the Ag2-O-N-O-Ag1 chains, thus forming a 2D network (Fig.1 and Fig. S10). The 2D network contains two types of 11- and 12-membered parallelogram-shaped units (Fig. S11). Ag–S–Ag–S–Ag chains run parallel, and the S–Ag–S angles are nearly equivalent with S1–Ag1–S1 and S2–Ag2–S2 angles of 133.64(2) and 133.14(2)°, respectively. **CP2** crystallizes in the monoclinic $P2_1/n$ space group (Tables S1, S3) and the asymmetric unit contains one silver ion, one **L2** molecule and one nitrate anion (Fig. S12).

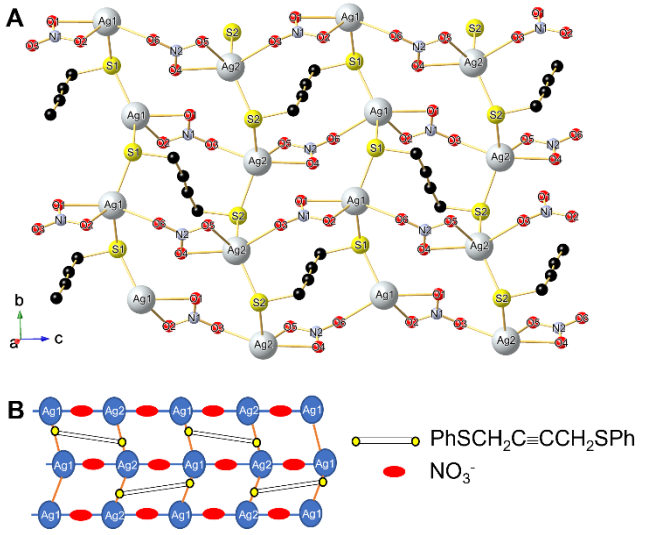

Fig. 1 (A) View of the 2D network of $[Ag_2\mathbf{L1}(NO_3)_2]_n$ (**CP1**). The H atoms and phenyl groups are omitted for clarity. (B) schematic representation of the 2D network of **CP1.**

In **CP2**, as in **CP1**, the silver atoms are five-coordinated to two S atoms from distinct **L2** ligands and 3 oxygen atoms from two different nitrate anions. Two nitrato groups bridge alternating silver atoms to form a polymeric Ag–O–N–O–Ag 1D chain extending in the *b* direction. The main difference between the two structures relies on the coordinating mode of the sulphur atoms. Contrary to **CP1**, in which each sulphur atom is acting as 4-electron donor, the sulphur atoms of **L2** in **CP2** acts as 2-electron donor. Also, **L2** now links two silver atoms of two Ag–O–N–O–Ag chains to form a 2D layer parallel to the *ab* plane (Fig.2 and S13). The mono (μ_2-S) coordination mode of the **L2** ligand led to an increase of the S1–Ag–S2 angle from ≈ 133° in **CP1** to 151.607(7)° in **CP2**. The 2D network contains just one type of 22-membered parallelogram-shaped units (Fig. S14). This framework is reminiscent to others obtained by reaction of $AgNO_3$ with phenyl-substituted dithioethers ligands such as trans-1,4-bis(phenylthio)-2-butene,[40] 1,10-bis(phenylthio)decane[41] and 1,4-bis(phenylthio)butane.[37] We are aware of only one example of a CP containing the same architecture with a cyclohexyl-substituted dithioether.[42] Table S4 compares Ag–S and Ag–O distances reported for these latter structures with those found in **CP2** and reveals that **CP2** presents the shortest Ag–S distances. Finally, in **CP2**, the averaged Ag–S distances are shorter than in **CP1.** This may be due to the different bonding modes between **L1** (4-electron donor) in **CP1** and **L2** being a 2-electron donor in **CP2** (mean *d*Ag–S distances 2.5534 Å in **CP1** *vs* 2.4737 Å in **CP2**) but also to the different electron-donor propensity of the cyclohexyl group (Table S4). As a result of this shortening/strengthening of the Ag–S bond the evolution of the Ag–O distance follows a reverse trend with an elongation of the mean Ag–O distance when going from **CP2** to **CP1** (mean Ag–O distance of 2.563 Å in **CP1** *vs*. 2.5978 Å in **CP2**). As for **CP1**, no close Ag…π contacts with the C≡C bond were evidenced for **CP2**. The antibacterial activities of **CP1** and **CP2** were first determined by means of their MIC/MBC (MIC = Minimal Inhibitory Concentration; MBC

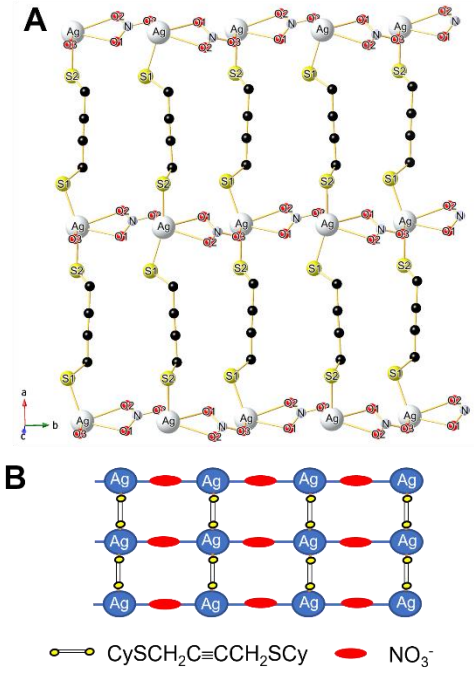

Fig.2 (A) View of the 2D network of $[Ag\mathbf{L2}(NO_3)]_n$ (**CP2**). The H atoms and cyclohexyl groups are omitted for clarity. B) schematic representation of the 2D network of **CP2**.

= Minimal Bactericidal Concentration) against Gram-negative *E. coli* and Gram-positive *S. aureus.* These two microorganisms belong to important human and animal pathogens and have been chosen as representatives of the main groups of infectious agents. Table 1 summarizes the obtained MICs values. For aqueous solution of $AgNO_3$, a MIC value of 5 µg $Ag.mL^{-1}$ was determined for both bacterial strains. For **L1** and **L2**, the highest concentrations tested were prepared by dissolution of the ligands in a mixture of water and acetonitrile (94:6 vol%), a composition that was checked to have no influence on bacteria growth. The antimicrobial activities of the free ligands were estimated as >80 $µg.mL^{-1}$ (i.e. the concentration on the first well) indicating no activity in the concentration range studied. MIC values of **CP1** and **CP2** were determined after dissolution in water/DMSO solutions (95/5% v/v) for the highest concentration. Here, again we have checked that this concentration has no influence on bacteria growth. Under these conditions, MICs values of **CP1** and **CP2** are identical both against *E. coli* (8 µg $Ag.mL^{-1}$) and against *S. aureus (5* µg $Ag.mL^{-1}$) and are close to MIC values of pure $AgNO_3$. Thioether-based CPs are known for their low solubility in most organic solvent so this surprising solubility might be due to complete decoordination of the ligands leading to the liberation of silver ions. This was confirmed by measuring the conductivities values of **CP1** and **CP2** in water/DMSO solutions (95/5% v/v) that are equal to the one obtained for $AgNO_3$ in the same solvent (σ = 154 $\mu S.cm^{-1}$). Therefore, MICs values were determined using suspensions of **CP1** and **CP2** in culture media. In this case, **CP1** and **CP2** still display good bacteriostatic activities against *E. coli* and *S. aureus* with identical MICs values. These MICs are twice and four times superior with respect to the ones determined using pure $AgNO_3$. Moreover, MIC values for **CP1** and **CP2** fall in the range reported in other studies on the antimicrobial activity of silver-based CPs especially against *E. coli.*[10, 43] **CP1** and **CP2** are of comparable activity as the commercially available topical antibiotic reference drug silver(I) sulfadiazine.[44] The MBCs values of **CP1** and **CP2** were also evaluated. Below MIC values, the total colony forming units (CFUs) found were always higher than 10^9 $CFU.mL^{-1}$ (i.e. the initial concentration of the bacterial inoculum). **CP1** and **CP2** have similar or close MIC and MBC values showing that these compounds present both bacteriostatic and bactericidal activity. The bactericidal activity of **CP1** and **CP2** was further studied by time-killing assays. To ensure that we only evaluated the bactericidal activity of our compounds, we used 100% phosphate-buffered saline (PBS) medium condition in which the quantity of CFUs remains constant during the whole procedure.

Table 1. MIC values (expressed in µg $Ag.mL^{-1}$) for studied compounds and MBC values for **CP1** and **CP2**.

Compound	*E. coli* ATCC 25922		*S. aureus* ATCC 25923	
	MIC	MBC	MIC	MBC
$AgNO_3$ in water	5	nd	5	nd
L1 (6% vol MeCN sol.)	> 80	nd	> 80	nd
L2 (6% vol MeCN sol.)	> 80	nd	> 80	nd
CP1 (5% vol DMSO sol.)	8	nd	5	nd
CP2 (5% vol DMSO sol.)	8	nd	5	nd
CP1 suspension	20	20	10	10
CP2 suspension	20	40	10	10

nd: non determined

These conditions were also chosen to link results of time-killing assays with those of silver release usually performed in 100% PBS. The tested concentrations are all below the MIC. Our results show that both CPs can entirely kill the bacteria within 1 to 8 hours, **CP2** being more efficient than **CP1** at equal concentration (Fig. 3a). As expected, increasing the CPs concentration from 1 to 10 µg $Ag.mL^{-1}$ results in a faster killing of the bacteria (8h for **CP1** at 1 µg $Ag.mL^{-1}$ (**CP1-1**) and 2h at 10 µg $Ag.mL^{-1}$ (**CP1-10**), 3h for **CP2** at 1 µg $Ag.mL^{-1}$ (**CP2-1**) and 1h at 10 µg $Ag.mL^{-1}$ (**CP2-10**). From Fig. 3b, it can be observed that the amount of silver ions released from PBS suspensions of **CP1** and **CP2** is always higher for **CP2** than **CP1**, regardless of the starting concentrations and that the highest CPs' concentration led to the highest quantity of silver released. Considering now the time intervals needed to kill all bacteria for each CP and each concentration (Fig. 3a), the amount of silver released at these times can be determined on Fig. 3b. For **CP1-10**, 0.55 µg $Ag.mL^{-1}$ are released while for **CP2-10** and **CP2-1** after 2 and 3 hours respectively, this amount is slightly higher than 0.2 µg $Ag.mL^{-1}$ and for **CP1-1** after 6 hours the amount released is slightly lower than 0.2 µg $Ag.mL^{-1}$. To determine the effect of such silver concentrations on *E. coli* survival under these conditions, we performed experiments using $AgNO_3$ as bactericidal agent in the concentration range (0.1-0.6 µg $Ag.mL^{-1}$) (Fig. 3c). Bacteria are completely killed within 1h using a solution of $AgNO_3$ at 0.6 µg $Ag.mL^{-1}$, within 2h at 0.3.µg $Ag.mL^{-1}$ and after 4h at 0.1 µg $Ag.mL^{-1}$. These killing assays match perfectly with the results found for **CP1** and **CP2** and clearly evidenced that the release of silver ions is responsible for the activity of our CPs. Finally, as demonstrated in the case of **CP1**, the activity is preserved when the media is replaced by a fresh one showing that our CPs act as reservoir that can be reused (Fig. 3d). Morphological changes of *E. coli* after contact with **CP1** suspensions were surveyed by Scanning Electron Microscopy (SEM). As shown in Fig. 4A, the untreated bacterium presents a solid rod shape with intact and smooth membrane. Addition of **CP1** at concentrations CMI/2 alters cell morphology (Fig. 4B) while at CMI and CMI×2, the cell membrane undergoes lysis (Fig. 4 C and D) associated with bacterial content leakage (dark area).

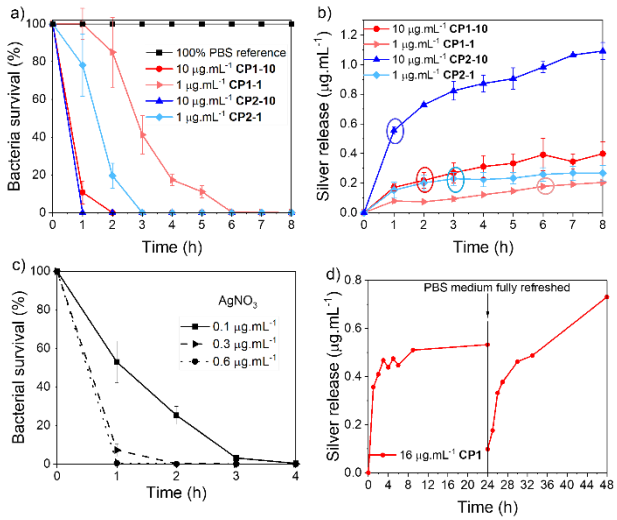

Fig 3 (a) % of surviving *E. coli* bacteria in PBS in the presence of **CP1** or **CP2** (b) silver released from **CP1** and **CP2** in PBS. (c) % of surviving bacteria in the presence of aqueous $AgNO_3$ solutions (d) silver released from **CP1** over 48h. The PBS medium was carefully removed and replaced by fresh PBS after 24h. Concentrations are given in µg $Ag.mL^{-1}$.

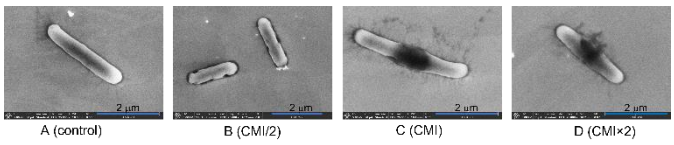

Fig.4 SEM Images of *E. coli* bacteria in the presence of **CP1** at different concentrations.

In summary, we reported the first examples on the antibacterial properties of CPs constructed from dithioethers ligands. Despite received ideas that antibacterial properties of CPs depend on their stability and that the latter can be deduced from HSAB principle, we demonstrate here that the combination soft donor ligands-soft Lewis acid is also efficient to elaborate antibacterial CPs. As solids, these CPs are stable for several months under ambient conditions and slowly release silver atoms when suspended in aqueous media. We performed simultaneous silver release and killing assays in PBS to confirm that the antibacterial properties are related to silver release. The lower activity of **CP1** with respect to **CP2** may be accounted to its higher chemical stability. Indeed, in **CP1**, **L1** acts as a 4-electron donor stabilizing the architecture. From the SEM images, the antimicrobial-mechanism of the Ag-CP may be ascribed to membrane disruption.

We acknowledge the French Renatech network and its FEMTO-ST technological facility and Marina Raschetti for her help in setting up the experiments with SEM-FEG.

Conflicts of interest

There are no conflicts to declare.

Notes and references

1. H. J. Klasen, *Burns*, 2000, **26**, 117-130.
2. A. B. G. Lansdown, *J. Wound Care*, 2002, **11**, 125-130.
3. S.-B. Miao, Z.-H. Li, C.-Y. Xu and B.-M. Ji, *CrystEngComm*, 2016, **18**, 4636-4642.
4. H.-Y. Shi, Y.-B. Dong, Y.-Y. Liu and J.-F. Ma, *CrystEngComm*, 2014, **16**, 5110-5120.
5. J. Chen, N. Voutier, J. Rajabi, A. Crochet, D. M. Bassani and K. M. Fromm, *CrystEngComm*, 2017, **19**, 5106-5113.
6. G.-P. Yang, Y.-Y. Wang, P. Liu, A.-Y. Fu, Y.-N. Zhang, J.-C. Jin and Q.-Z. Shi, *Cryst. Growth Des.*, 2010, **10**, 1443-1450.
7. M. Gutierrez, C. Martin, B. E. Souza, M. Van der Auweraer, J. Hofkens and J. C. Tan, *Appl. Mater. Today*, 2020, **21**.
8. A. Tabacaru, C. Pettinari, F. Marchetti, C. di Nicola, K. V. Domasevitch, S. Galli, N. Masciocchi, S. Scuri, I. Grappasonni and M. Cocchioni, *Inorg. Chem.*, 2012, **51**, 9775-9788.
9. K. M. Fromm, *Appl. Organomet. Chem.*, 2013, **27**, 683-687.
10. X. Y. Lu, J. W. Ye, Y. Sun, R. F. Bogale, L. M. Zhao, P. Tian and G. L. Ning, *Dalton Trans.*, 2014, **43**, 10104-10113.
11. G. Wyszogrodzka, B. Marszalek, B. Gil and P. Dorozynski, *Drug Discov. Today*, 2016, **21**, 1009-1018.
12. M. F. Shen, F. Forghani, X. Q. Kong, D. H. Liu, X. Q. Ye, S. G. Chen and T. Ding, *Compr. Rev. Food Sci. Food Saf*, 2020, **19**, 1397-1419.
13. R. Li, T. Chen and X. Pan, *ACS Nano*, 2021, **15**, 3808-3848.
14. W. Q. Nong, J. Wu, R. A. Ghiladi and Y. G. Guan, *Coord. Chem. Rev.*, 2021, **442**.
15. W. Zhang, G. Ye, D. Liao, X. Chen, C. Lu, A. Nezamzadeh-Ejhieh, M. S. Khan, J. Liu, Y. Pan and Z. Dai, *Molecules*, 2022, **27**, 7166.
16. K. Akhbari, M. Hemmati and A. Morsali, *J. Inorg. Organomet. Polym.*, 2011, **21**, 352-359.
17. J. S. Jung, S. J. Ko, H. B. Lee, S. B. Lee, H. J. Kim and J. M. Oh, *Polymers*, 2019, **11**.
18. Z. R. Ranjbar and A. Morsali, *Synth. Met.*, 2011, **161**, 1449-1455.
19. K. Nomiya, K. Tsuda, T. Sudoh and M. Oda, *J. Inorg. Biochem.*, 1997, **68**, 39-44.
20. K. Nomiya, K.-I. Onoue, Y. Kondoh, N. C. Kasuga, H. Nagano, M. Oda and S. Sakuma, *Polyhedron*, 1995, **14**, 1359-1367.
21. K. Nomiya, S. Takahashi, R. Noguchi, S. Nemoto, T. Takayama and M. Oda, *Inorg. Chem.*, 2000, **39**, 3301-3311.
22. C. Pettinari, R. Pettinari, C. Di Nicola, A. Tombesi, S. Scuri and F. Marchetti, *Coord. Chem. Rev.*, 2021, **446**, 214121.
23. R. G. Pearson and J. Songstad, *J. Am. Chem. Soc.*, 1967, **89**, 1827-1836.
24. S. C. Chen, Z. H. Zhang, Q. Chen, L. Q. Wang, J. Xu, M. Y. He, M. Du, X. P. Yang and R. A. Jones, *Chem. Commun.*, 2013, **49**, 1270-1272.
25. X. Y. Lu, J. W. Ye, D. K. Zhang, R. X. Xie, R. F. Bogale, Y. Sun, L. M. Zhao, Q. Zhao and G. L. Ning, *J. Inorg. Biochem.*, 2014, **138**, 114-121.
26. A. Tăbăcaru, C. Pettinari, M. Bușilă and R. M. Dinică, *Polymers*, 2019, **11**, 1686.
27. G. Ahadiat, M. Tabatabaee, K. Gholivand, K. Zare and M. Dusek, *J. Coord. Chem.*, 2021, **74**, 1057-1065.
28. J. M. S. Cardoso, A. M. Galvao, S. I. Guerreiro, J. H. Leitao, A. C. Suarez and M. Carvalho, *Dalton Trans.*, 2016, **45**, 7114-7123.
29. R. J. Young, S. L. Begg, C. J. Coghlan, C. A. McDevitt and C. J. Sumby, *Eur. J. Inorg. Chem.*, 2018, 3512-3518.
30. X. Y. Yu, R. Zhang, S. L. Li, S. H. Yu, L. Gao, W. F. Yan, J. Jin and Y. N. Luo, *Inorg. Chem. Commun.*, 2020, **116**.
31. S. Kulovi, S. Dalbera, S. K. Dey, S. Maiti, H. Puschmann, E. Zangrando and S. Dalai, *Chemistryselect*, 2018, **3**, 5233-5242.
32. I. Chevrier, J. L. Sague, P. S. Brunetto, N. Khanna, Z. Rajacic and K. M. Fromm, *Dalton Trans.*, 2013, **42**, 217-231.
33. L. Viau, M. Knorr, L. Knauer, L. Brieger and C. Strohmann, *Dalton Trans.*, 2022, **51**, 7581-7606.
34. A. Raghuvanshi, M. Knorr, L. Knauer, C. Strohmann, S. Boullanger, V. Moutarlier and L. Viau, *Inorg. Chem.*, 2019, **58**, 5753-5775.
35. J. Y. Lee, S. Y. Lee, W. Sim, K.-M. Park, J. Kim and S. S. Lee, *J. Am. Chem. Soc.*, 2008, **130**, 6902-6903.
36. A. Schlachter, K. Tanner and P. D. Harvey, *Coord. Chem. Rev.*, 2021, **448**, 214176.
37. X.-H. Bu, W. Chen, W.-F. Hou, M. Du, R.-H. Zhang and F. Brisse, *Inorg. Chem.*, 2002, **41**, 3477-3482.
38. X. H. Bu, W. F. Hou, M. Du, W. Chen and R. H. Zhang, *Cryst. Growth Des.*, 2002, **2**, 303-307.
39. R. Q. Zou, J. R. Li, Y. B. Xie, R. H. Zhang and X. H. Bu, *Cryst. Growth Des.*, 2004, **4**, 79-84.
40. Y. Zheng, J.-R. Li, M. Du, R.-Q. Zou and X.-H. Bu, *Cryst. Growth Des.*, 2005, **5**, 215-222.
41. M. O. Awaleh, A. Badia, F. Brisse and X.-H. Bu, *Inorg. Chem.*, 2006, **45**, 1560-1574.
42. T. H. Kim, Y. W. Shin, K.-M. Park and J. Kim, *Acta Cryst. E*, 2009, **65**, m385.
43. F. Marchetti, J. Palmucci, C. Pettinari, R. Pettinari, S. Scuri, I. Grappasonni, M. Cocchioni, M. Amati, F. Lelj and A. Crispini, *Inorg. Chem.*, 2016, **55**, 5453-5466.
44. J. M. T. Hamilton-Miller, S. Shah and C. Smith, *Chemotherapy*, 1993, **39**, 405-409.